

THE COLLAPSE MECHANISM OF A SOIL SUBJECTED TO ONE-DIMENSIONAL LOADING AND WETTING

D. G. FREDLUND AND J. K-M. GAN
Professor of Civil Engineering and Research Engineer, respectively
University of Saskatchewan, Saskatoon, Saskatchewan, Canada
S7N 0W0

ABSTRACT

Matric suction can be used as one of the principal stress state variable to define the constitutive behavior of collapsing soils. The collapse behavior of a compacted soil was studied in the laboratory using a modified conventional oedometer and a tensiometer for the measurement of matric suction. The results show that collapse is a transient, continuous process. The results were used to model the volume change of a collapsible soil during wetting. The theoretical formulations derived for the model were based on unsaturated soil mechanics principles. Results obtained from the numerical model compared well with the laboratory measurements.

1. Introduction

There are different types of soils found in nature which collapse under certain conditions. These soils can be broadly divided into two groups; namely, wet collapsible soils and dry collapsible soils (also known as hydrocollapsible soils). Wet collapsible soils such as quick clays found in Eastern Canada and in Scandinavian countries can exist in a stable condition under high *insitu* water contents. Naturally occurring dry collapsible soils may be cemented or uncemented. This paper deals only with *uncemented, dry collapsible* soils which may be remolded (i.e., laboratory compacted) or found in an undisturbed state in nature.

A mechanical disturbance which induces a shear stress is the triggering mechanism in the collapse of wet collapsible soils. The collapse occurs with no change in the water content of the soil. The triggering mechanism in an uncemented, dry collapsible soils is attributable to the loss of strength due to a reduction in matric suction as a result of wetting (i.e., a loss in normal stress between particles leading to shear failure). In other words, an uncemented, dry collapsible soil collapses when there is a change in the stress state of the soil as it goes from an unsaturated condition towards a saturated condition. The principles of unsaturated soil mechanics appear to provide a

reasonable framework for the characterization of the behavior of uncemented, dry collapsible soils.

The objectives of this paper are to illustrate the collapse mechanism of an uncemented, dry collapsible soil and to show the applicability of unsaturated soil mechanics principles in describing the collapse behavior. The scope of the paper will be limited to an uncemented, dry collapsible soil. The term collapsible soil will be taken to mean an uncemented, dry collapsible soil for the remainder of this paper.

Much of the information presented is synthesized from papers by Tadealli and Fredlund (1991), Tadealli, Fredlund and Rahardjo (1992) and Tadealli, Rahardjo and Fredlund (1992). The experimental work was conducted by Tadealli (1990) as part of his thesis at the University of Saskatchewan, Saskatoon, Saskatchewan, Canada.

2. Unsaturated Soil Mechanics Framework for Collapsible Soils

Fredlund and Morgenstern (1977) provided the theoretical and experimental justifications for the use of two independent stress-state variables, (i.e., $(\sigma - u_a)$ and $(u_a - u_w)$ where σ = normal stress, u_a = pore-air pressure and u_w = pore-water pressure), for characterizing the behavior of unsaturated soils. The characterization can also be shown to include the behavior of dry collapsible soils.

2.1 VOLUME CHANGE FORMULATIONS

The compressibility form of the constitutive equation for the one-dimensional soil structure volume change of a saturated soil is written as:

$$\frac{dV_v}{V_o} = m_v d(\sigma_y - u_w) \quad (1)$$

where

dV_v = change in total volume

V_o = initial total volume

m_v = coefficient of volume change

$d(\sigma_y - u_w)$ = change in effective stress.

In Eq. (1), the deformation state variable, dV_v / V_o , is related to the stress state variable, $(\sigma_y - u_w)$, by a soil property, m_v , known as the coefficient of volume

change. The stress state variable, (i.e., $(\sigma_y - u_w)$), is known as effective stress when dealing with saturated soils.

Equation (1) can be similarly extended to describe the deformation of an unsaturated soil by relating the deformation state variable, dV_v / V_o , to the two stress state variables (i.e., $(\sigma_y - u_a)$ and $(u_a - u_w)$). The resulting compressibility form of the constitutive relationship for the one-dimensional volume change of the soil structure in an unsaturated soil is written as,

$$\frac{dV_v}{V_o} = m_1^s d(\sigma_y - u_a) + m_2^s d(u_a - u_w) \quad (2)$$

where

$$m_1^s = \text{coefficient of volume change with respect to a change in net normal stress, } d(\sigma_y - u_a)$$

$$m_2^s = \text{coefficient of volume change with respect to a change in matric suction, } d(u_a - u_w).$$

Similarly, an independent, water phase volume change equation can be written for an unsaturated soil,

$$\frac{dV_w}{V_o} = m_1^w d(\sigma_y - u_a) + m_2^w d(u_a - u_w) \quad (3)$$

where

$$dV_w = \text{change in volume of water,}$$

$$m_1^w = \text{coefficient of water volume change with respect to a change in net normal stress, } d(\sigma_y - u_a)$$

$$m_2^w = \text{coefficient of water volume change with respect to a change in matric suction, } d(u_a - u_w).$$

A similar equation can also be written for the change in volume of air in the soil. The continuity requirement shows that the third deformation state variable for the air phase can be computed from the deformation state variables of the soil structure and the water phase. The continuity requirement is given by the equation:

$$\frac{\Delta V_v}{V_o} = \frac{\Delta V_w}{V_o} + \frac{\Delta V_a}{V_o} \quad (4)$$

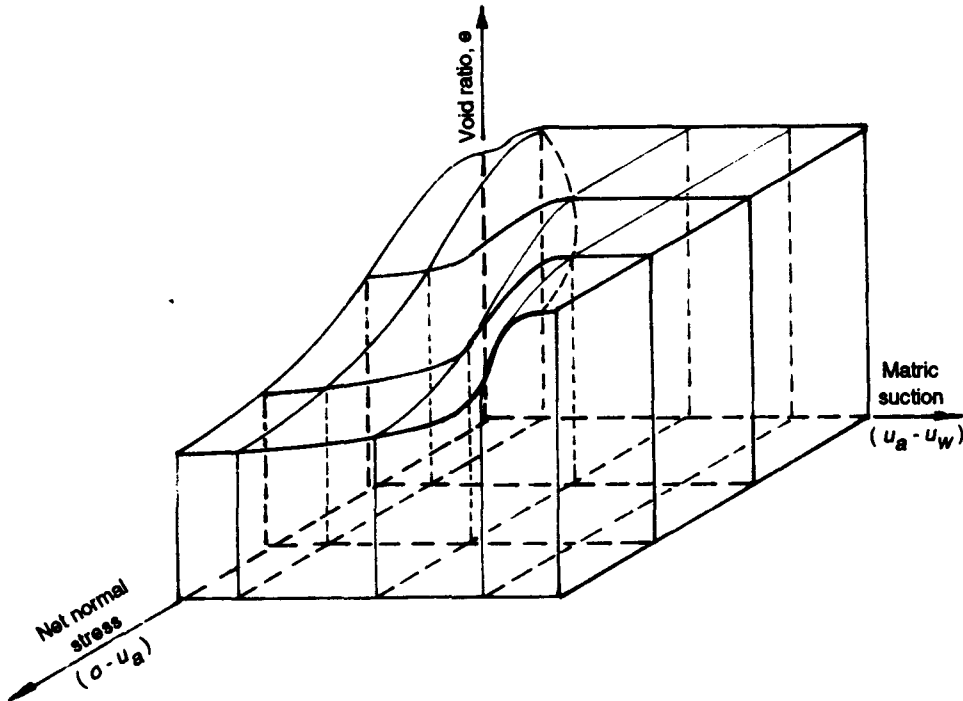


Figure 1. Soil structure constitutive surface for an uncemented, collapsible unsaturated soil in terms of void ratio.

The corresponding constitutive surface for the deformation states of a collapsible soil in terms of the void ratio, e (where $e = V_v / V_s$ and V_v , V_s are the volume of voids and the volume of solids, respectively), is presented in Fig. 1.

2.2 FLOW FORMULATIONS

The collapse of an unsaturated soil involves the inflow of water into the soil. There are two fluid phases involved in the flow problem. There is a net inflow of water and a net outflow of air. However, the formulation can be simplified by assuming that the dissipation of excess pore-air pressure is instantaneous. The problem is then reduced to one of water flow. The interested reader can refer to Fredlund and Rahardjo (1993) for the formulation of two-phase flow analysis.

2.2.1 Derivation of Water Phase Partial Differential Equation

Consider one-dimensional water flow through a differential element of unsaturated collapsible soil as shown in Fig. 2. From the principle of the conservation of mass, the net flux of water through the element can be computed from the volume of water entering and leaving the element within any given period of time.

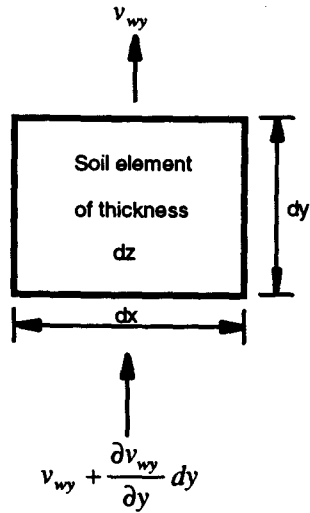


Figure 2. One-dimensional transient flow of water into a collapsible soil element.

$$\frac{\partial V_w}{\partial t} = \left(v_w + \frac{\partial v_w}{\partial y} dy \right) dx dz - v_w dx dz \quad (5)$$

where

∂V_w = change in the volume of water in the soil element over a specific time, ∂t

$\partial V_w / \partial t$ = net flux of water through the soil element

v_w = water flow rate across a unit area of the soil element in the y -direction

dx, dy, dz = infinitesimal dimensions of the element in the x -, y - and z -directions, respectively.

Expressing the net flux of water in terms of a unit volume of soil and rearranging Eq. (5) yields:

$$\frac{\partial (V_w / V_o)}{\partial t} = \frac{\partial v_w}{\partial y} \quad (6)$$

where

V_o = initial volume of soil element (i.e., $dx dy dz$)

Substituting Darcy's law for the flow rate of water, v_w , into Eq. (6) gives:

$$\frac{\partial(V_w / V_o)}{\partial t} = \frac{\partial\left(-k_w \frac{\partial h_w}{\partial y}\right)}{\partial y} \quad (7)$$

where

k_w = coefficient of permeability for the water phase as a function of matric suction

h_w = hydraulic head (i.e., gravitational plus pore-water pressure head or $y + (u_w / \rho_w g)$)

y = elevation

u_w = pore-water pressure

ρ_w = density of water

g = gravitational acceleration

$\partial h_w / \partial y$ = hydraulic head gradient in the y -direction.

Rearranging Eq. [7] gives:

$$\frac{\partial(V_w / V_o)}{\partial t} = -k_w \frac{\partial^2 h_w}{\partial y^2} - \frac{\partial k_w}{\partial y} \frac{\partial h_w}{\partial y} \quad (8)$$

Substituting $(y + u_w / \rho_w g)$ for h_w in Eq. (8):

$$\frac{\partial(V_w / V_o)}{\partial t} = -k_w \frac{\partial^2\left(y + \frac{u_w}{\rho_w g}\right)}{\partial y^2} - \frac{\partial k_w}{\partial y} \frac{\partial\left(y + \frac{u_w}{\rho_w g}\right)}{\partial y} \quad (9)$$

which reduces to,

$$\frac{\partial(V_w / V_o)}{\partial t} = -\frac{k_w}{\rho_w g} \frac{\partial^2 u_w}{\partial y^2} - \frac{1}{\rho_w g} \frac{\partial k_w}{\partial y} \frac{\partial u_w}{\partial y} - \frac{\partial k_w}{\partial y} \quad (10)$$

The water phase constitutive relation given earlier by Eq. (3) defines the change in the volume of water in a soil element caused by the changes in the net normal stress, $(\sigma_y - u_a)$, and the matric suction, $(u_a - u_w)$. The flux of water flow per unit volume of the soil can be obtained by differentiating the water phase constitutive relation [Eq. (3)] with respect to time:

$$\frac{\partial(V_w / V_o)}{\partial t} = m_1^w \frac{\partial(\sigma_y - u_a)}{\partial t} + m_2^w \frac{\partial(u_a - u_w)}{\partial t} \quad (11)$$

Both equations for the flux of water [i.e., Eq. (10) and Eq. (11)] can now be equated to give the partial differential equation for the water phase:

$$m_1^w \frac{\partial \sigma_y}{\partial t} - m_1^w \frac{\partial u_a}{\partial t} + m_2^w \frac{\partial u_a}{\partial t} - m_2^w \frac{\partial u_w}{\partial t} = - \frac{k_w}{\rho_w g} \frac{\partial^2 u_w}{\partial y^2} - \frac{1}{\rho_w g} \frac{\partial k_w}{\partial y} \frac{\partial u_w}{\partial y} - \frac{\partial k_w}{\partial y} \quad (12)$$

Collapse usually occurs at constant applied stress condition (i.e., $\sigma_y = \text{constant}$). Therefore, the change in total stress with respect to time can be set to zero (i.e. $\partial \sigma_y / \partial t = 0$). The resulting differential equation for the water phase can be written as follows:

$$\frac{\partial u_w}{\partial t} = - C_w \frac{\partial u_a}{\partial t} + c_v^w \frac{\partial^2 u_w}{\partial y^2} + \frac{\partial c_v^w}{\partial y} \frac{\partial u_w}{\partial y} + c_g \frac{\partial k_w}{\partial y} \quad (13)$$

where

C_w = interactive constant associated with the water phase partial differential equation, i.e. $[(1 - m_2^w / m_1^w) / (m_2^w / m_1^w)]$

c_v^w = coefficient of consolidation with respect to the water phase (i.e., $k_w / (\rho_w g m_2^w)$)

c_g = gravity term constant (i.e., $1 / m_2^w$)

The last term on the right hand side of Eq. (13) (i.e., $c_g \partial k_w / \partial y = (1 / m_2^w) (\partial k_w / \partial y)$) is the result of the inclusion of the gravitational component of the hydraulic head. In many cases, this term can be taken as negligible when compared to other terms. For example, in the study of the infiltration of water into a dry soil with a high initial matric suction, the gravitational component of the hydraulic head may be relatively small when compared with the head associated with the matric suction component.

The coefficient of permeability of soil with respect to air is usually much higher than the coefficient of permeability of soil with respect to water, particularly in a loose-structured collapsible soil. It may be assumed that any excess pore-air pressure would be dissipated almost instantaneously through released from the system as free air. Therefore, the transient process associated with the water phase alone controls behavior. Neglecting also the gravitational component, $c_g \partial k_w / \partial y$, the differential water flow equation can then be simplified to:

$$\frac{\partial u_w}{\partial t} = c_v^w \frac{\partial^2 u_w}{\partial y^2} + \frac{\partial c_v^w}{\partial y} \frac{\partial u_w}{\partial y} \quad (14)$$

Equation (14) can be expressed in an explicit finite difference form using the grid layout shown in Fig. 3.

$$u_{w(i,j+1)} = u_{w(i,j)} + \frac{\Delta t}{2\Delta y} \left[\left(c_{v(i+1,j)}^w u_{w(i+1,j)} \right) + \left(c_{v(i,j)}^w u_{w(i-1,j)} \right) - \left(c_{v(i,j)}^w u_{w(i,j)} \right) - \left(c_{v(i+1,j)}^w u_{w(i,j)} \right) \right] \quad (15)$$

A computer program can be written for Eq. (15) to predict changes in pore-water pressure with respect to time and depth subsequent to infiltration due to inundation. The changes in pore-water pressure can be substituted into Eq. (2) in order to compute the associated total volume change.

2.3 COMPARISON BETWEEN COLLAPSE AND CONSOLIDATION

The flow equations developed in the previous section for collapse behavior are the same equations which have been developed for consolidation and also for swelling in an unsaturated soil (Fredlund and Rahardjo, 1993). However, the flow processes associated with collapse and swell are fundamentally different from the flow processes associated with consolidation.

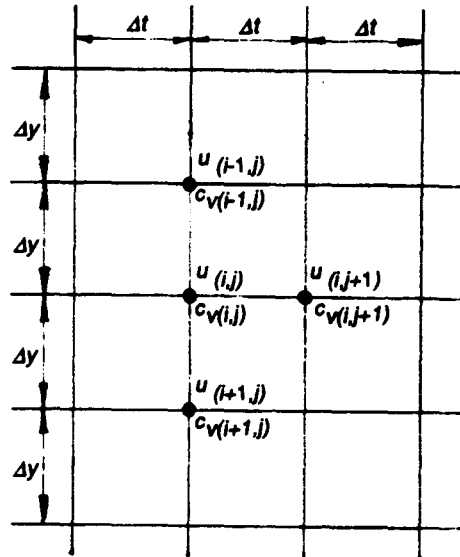


Figure 3. Grid and variables used in the finite-difference scheme.

The consolidation of an unsaturated soil involves the dissipation of excess pore pressures which are generally the result of an increase in the total stress. The dissipation of excess pore pressures results in the redistribution and/or outflow of water and air with time. The transient flow process is ubiquitous throughout the soil. Flow initiates throughout the entire soil profile. The water pressure head gradient, $(\partial u_w / \partial y)$, decreases gradually with time throughout the soil profile and the soil undergoes a gradual change in total volume. The change in the water content of the entire soil column undergoing consolidation is gradual. Typical pore-water pressure isochrones in a soil undergoing consolidation are shown in Fig. 4.

In collapse (as well as in swell), the water infiltrates into the interior of the soil, starting at the exterior boundaries. A collapsible soil generally has an open structure. An open-structured soil has a steep coefficient of permeability function. Infiltration into an open-structured soil with a steep coefficient of permeability function gives rise to a wetting front. The pressure head gradient is very steep at the wetting front and is low elsewhere away from the wetting front. It has been found that for a column of uniform soil with an initial constant matric suction profile subjected to ponding, the wetting front moves at approximately constant velocity (Bear, 1972). Figure 5 shows the water content and water pressure head profiles due to rainpond infiltration in an initially air dry sand (Rubin, 1966).

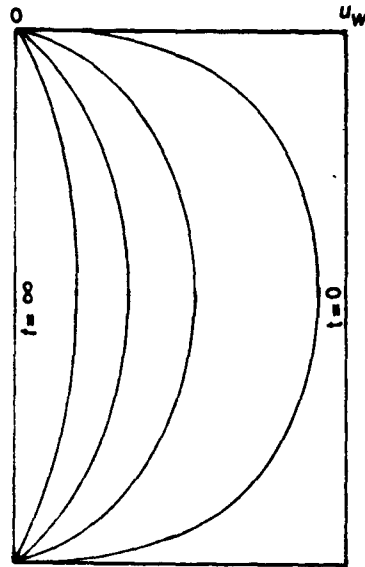


Figure 4. Typical isochrones in a consolidation process of a soil specimen which is drained at both ends.

In the collapse process, volume changes are predominantly confined within the wetted zone. The decrease in total volume due to the collapse of the soil within the wetted zone increases the local volumetric water content. The resulting matric suction

isochrones are similar to those in the infiltration process presented in Fig. 5. The high pressure gradient at the wetting front, the increase in volumetric water content of the collapse zone and the high air coefficient of permeability of the soil can be used to explain the rapid rate of collapse often observed.

The collapse of a soil can be analyzed in a manner similar to the consolidation of a soil. The total specimen undergoing collapse is analogous to the volume change in a consolidation process. During collapse, the sample reduces in volume as the matric suction is reduced, just as a sample undergoing consolidation reduces in volume as the pore-water pressure is reduced.

The advancing wetting front in a collapsing soil can be numerically modeled by using a suitable coefficient of permeability function. The advancing wetting front moves at a velocity dependent on the coefficient of permeability function for the soil.

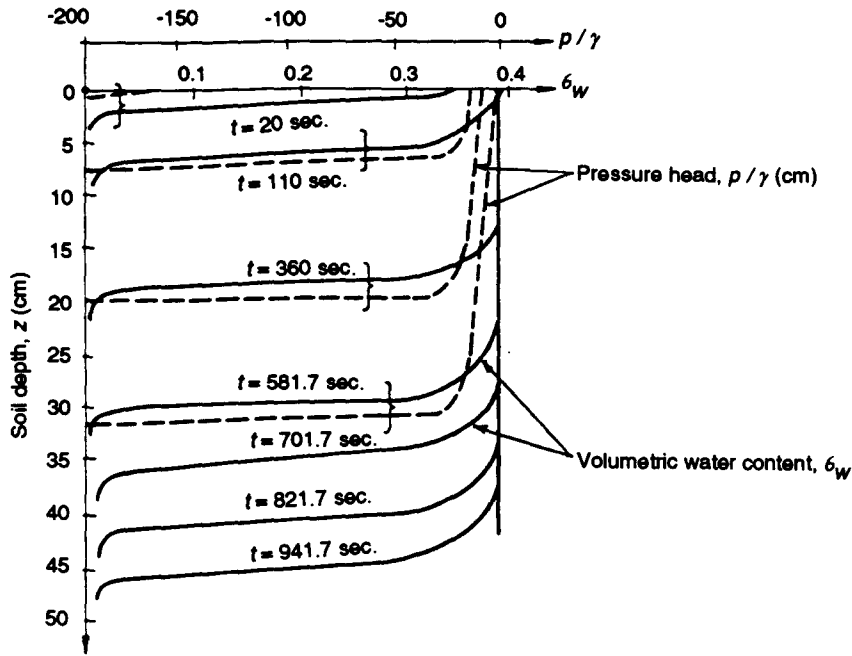


Figure 5. Water content and pressure head profiles during infiltration in an air-dry sand (Rubin, 1966).

With a steep coefficient of permeability function, the permeability increases from an initial low value to the saturated value as a result of a relatively small range of matric suction changes. Steep coefficient of permeability functions are characteristic of coarse soils and soils with a loose, open structure. Steep permeability functions, however, can produce great numerical instability in numerical simulations. Examples of typical coefficient of permeability functions obtained using Gardner's equation are shown in Fig. 6. Gardner's equation is given as Eq. (16) below.

$$k_w(u_a - u_w) = \frac{k_s}{1 + a \left(\frac{u_a - u_w}{\rho_w g} \right)^n} \quad (16)$$

where

$k_w(u_a - u_w)$ = coefficient of water phase permeability as a function of matric suction, $(u_a - u_w)$

k_s = coefficient of water phase permeability at saturation

a = soil constant which is a function of the air entry value of the soil

n = slope of k_w versus $(u_a - u_w)$ in the log-log plot of k_w versus $(u_a - u_w)$, beyond the air entry value.

The character of the coefficient of permeability function in Eq. (16) is defined by the a and n constants.

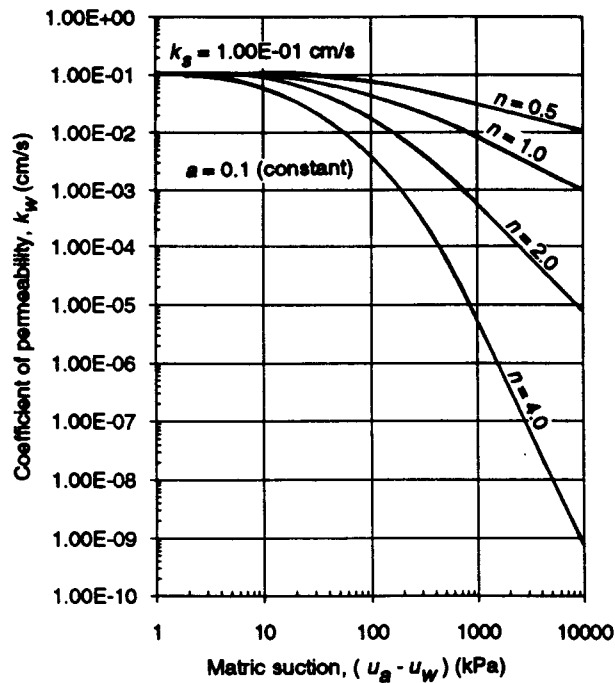


Figure 6. Water coefficient of permeability as a function of the matric suction using Gardner's equation.

3. Experimental Program

A two part laboratory test program was conducted to study the collapse of a statically compacted silt from the Indian Head region of Saskatchewan (Tadepalli, 1990). The index properties of the Indian Head silt are shown in Table 1.

The tests in Part One of the program were conducted to study the effects of initial dry density and water content on collapsibility. In Part Two of the program, tests were conducted to study the mechanism of collapse as the initial matric suction of the unsaturated compacted silt was reduced. The matric suction was reduced as result of infiltration from inundation.

3.1 PART ONE OF THE TEST PROGRAM

Three series of tests were conducted in Part One of the test program. In test Series No. 1, four oedometer tests were conducted on specimens which were each compacted to a dry density of about 1.6 Mg/m^3 at water contents of 7%, 10%, 14% and 18%, respectively.

TABLE 1. Summary of index properties for Indian Head Silt

Grain -size distribution	
Sand	62%
Silt	32%
Clay	6%
D_{10}	0.0034 mm
D_{30}	0.025 mm
D_{60}	0.090 mm
Coefficient of uniformity,	
$C_u = D_{60} / D_{10}$	26.4
Atterberg limits	
Liquid limits, w_L	22.2%
Plastic limits, w_P	16.6%
Plasticity index, PI	5.6%
Relative density, G_s	2.68

Test Series No. 2 involved eight oedometer tests. Four oedometer tests were conducted on specimens which were each compacted at a constant water content of 7% to initial dry densities of 1.4, 1.5, 1.6 and 1.65 Mg/m^3 , respectively. The next set of four oedometer tests were conducted on specimens which were each compacted at a constant water content of 12% to initial dry densities of 1.4, 1.5, 1.6 and 1.65 Mg/m^3 , respectively.

Test Series No. 3 involved six oedometer tests which were conducted on "identical" specimens. The specimens were compacted to the same initial dry density of 1.4 Mg/m^3 at an initial water content of 7.1%. The dry density value of 1.4 Mg/m^3 and an initial water content of 7.1% corresponds to the condition for maximum collapse which was determined from the results of test Series No. 1 and 2. One specimen each was tested in the as-compacted state and in the saturated state in the oedometer, respectively. The remaining four specimens were subjected to inundation at vertical stresses corresponding to 55 kPa, 222 kPa, 392 kPa and 811 kPa, respectively.

3.2 PART TWO OF THE TEST PROGRAM

Two series of tests were conducted in this part of the program. Test Series No. 4 consisted of three tests, S1M, S2M and S3M. An oedometer ring with a 7.5 mm hole at mid-height to accommodate a flexible tube type tensiometer (Fig. 7) was used for the tests. The height and diameter of the oedometer ring were 25.4 mm and 63.0 mm (Fig. 8a), respectively.

The dry density, water content and the vertical stress at inundation for the three specimens in tests S1M, S2M and S3M are summarized in Table 2.

TABLE 2. Summary of index properties and total pressure at inundation

Description	Test identification			
	S1M	S2M	S3M	S4M
Dry density, ρ_d (t / m^3)	1.598	1.506	1.405	1.394
Water content, w (%)	11.80	11.79	11.80	12.75
Vertical pressure at inundation(kPa)	97	96	99	55

One test was conducted in Series No. 5. The test S4M was conducted on a compacted specimen in an oedometer ring with a height and diameter of 60.0 mm and 84.9 mm, respectively (Fig. 8b). The oedometer ring had three 7.5 mm holes to accommodate three flexible tube type tensiometers. Two holes were located at a distance of 12.5 mm from the top and bottom of the ring. The third hole was located at mid-height of the ring. The dry density, water content and the vertical stress at inundation of the specimen in test S4M are shown in Table 2.

3.3 TEST PROCEDURES

The collapse tests in Part One were conducted in a conventional oedometer. In each test, the specimen was placed between two air dry porous stones in the oedometer ring. The oedometer set up was covered with plastic wrap to minimize moisture loss and was left for 24 hours.

After the 24 hour period, the specimen was loaded every 2 hours by doubling the previous load. When settlement under the applied load was complete, the specimen was inundated with distilled water. Subsequent to saturation of the specimen for 24 hours, further loads were again applied to the specimen under saturated conditions.

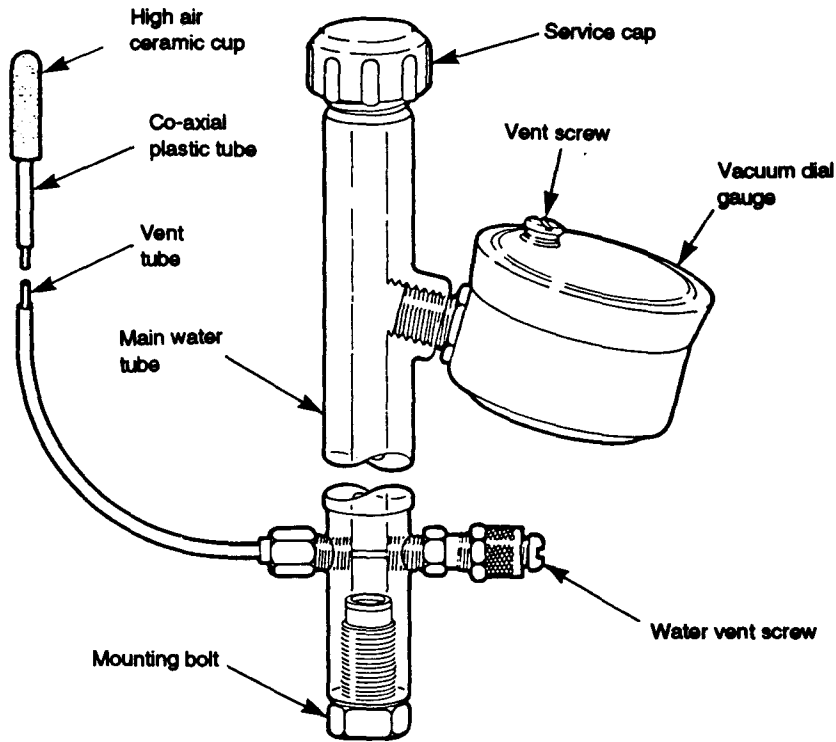


Figure 7. Small tip flexible tube type tensiometer (from Soil Moisture Equipment Corporation).

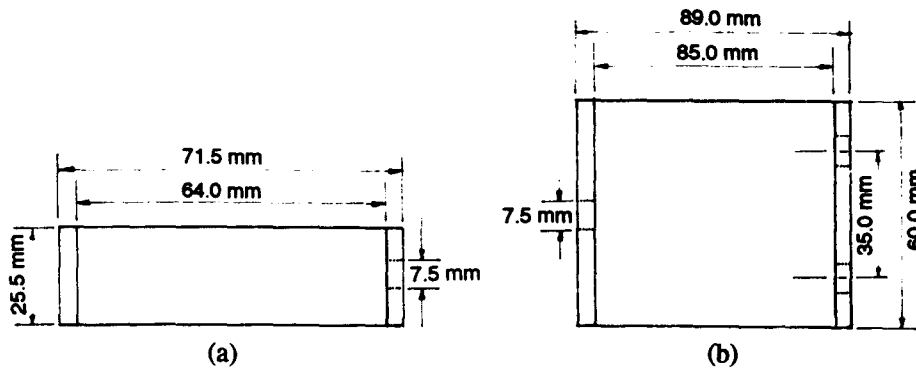


Figure 8. Modified oedometer rings used in the collapse tests; (a) for tests S1M, S2M and S3M, (b) for test S4M.

The collapse tests in Part Two were conducted in the modified oedometers with a tensiometer installed for matric suction measurements. The specimen was placed between two air dry porous stones and assembled in the oedometer equipment. The oedometer pot with specimen in place was covered with plastic wrap and was left until the tensiometer reading came to equilibrium. After the tensiometer reading has come to equilibrium, the specimen was loaded every two hours by doubling the previous load.

After settlement was complete under the selected applied vertical load, the specimen was inundated. In test series No. 4, water could flow into the specimen through both the top and bottom porous stones. In test Series No. 5, the specimen was allowed access to water only through the bottom porous stone. Throughout the wetting process, the tensiometer readings and the dial gauge readings were recorded simultaneously with time until the matric suction reading of the specimen decreased to zero. The final settlement at the end of 24 hours of wetting was recorded and the specimen was unloaded.

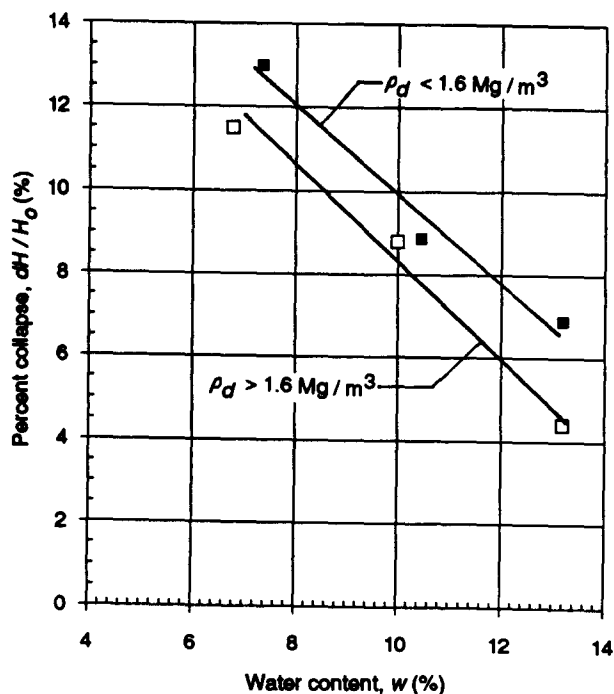


Figure 9. Effect of initial water content on the amount of collapse.

4. Test Results and Discussions

A summary of the results of tests from Part One of the program are presented in Figs. 9, 10 and 11. The results in Fig. 9 indicate that the amount of collapse decreases linearly with initial water content for specimens statically compacted at a constant initial dry density. Similarly, the results presented in Fig 10. indicate that the amount of collapse decreases linearly with initial dry density for specimens statically compacted at a constant water content.

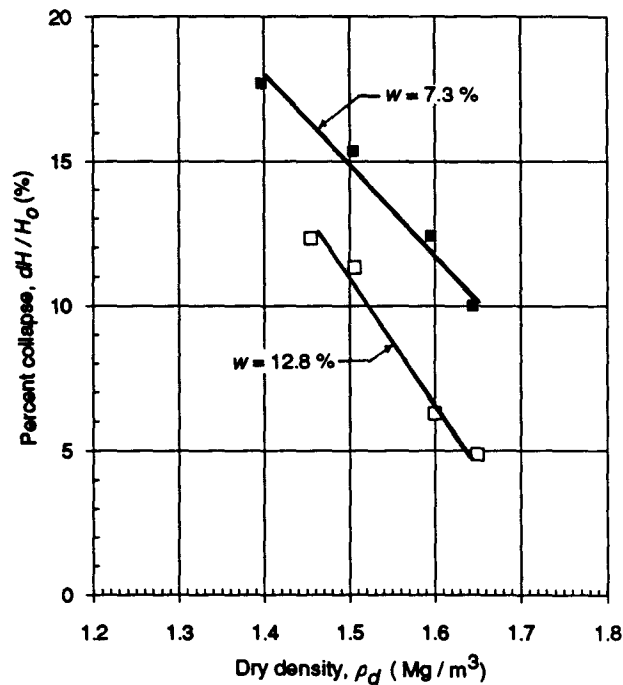


Figure 10. Effect of initial dry density on the amount of collapse.

The results of void ratio changes with vertical load in Fig. 11, for specimens inundated at various vertical loads, indicate that the void ratio changes due to inundation can be quite well predicted using the double oedometer approach. The results show that the void ratios of the initially unsaturated specimens approach the consolidation line of the saturated specimen after being subjected to inundation. The agreement appears to be superior for inundation at lower applied vertical loads.

The rebound curves for all six specimens in Fig. 11 are relatively flat, with close to zero or slightly negative slopes. It would appear that subsequent to collapse, the soil still exists in a state that is "loose" (i.e., high void ratios) with respect to the applied vertical stress.

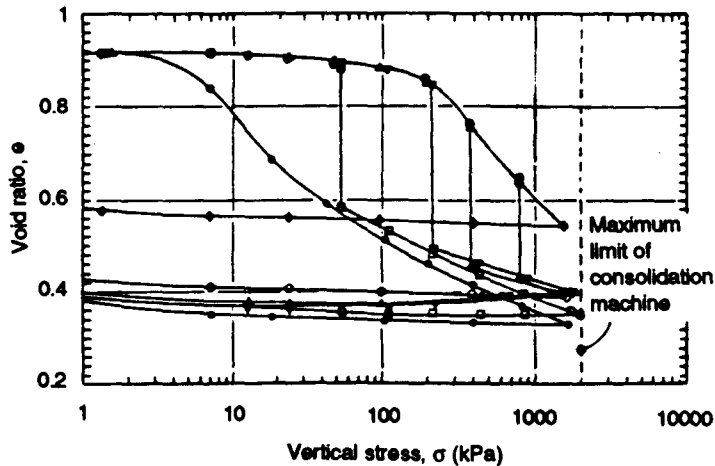


Figure 11. Effect of vertical pressure on the amount of collapse.

Changes in the matric suction at mid-height of the specimen and the changes in the total volume with time during inundation for tests, S1M, S2M and S3M, are presented in Figs. 12, 13 and 14. The results obtained from tests S1M, S2M and S3M (Figs. 12, 13 and 14) indicate that the initial matric suction of the specimens prior to inundation were 60, 58 and 64 kPa, respectively. All three specimens had an initial water content of around 12.0%. These initial values of matric suction are consistent with the results of pressure plate tests conducted on a statically compacted specimen with a dry density of 1.4 Mg / m^3 . The Soil-Water Characteristic Curve from the pressure plate test, presented in Fig. 15, shows that an initial water content of 12.0 % corresponds approximately to an initial matric suction of about 60 kPa.

The results of test S1M in Fig. 12 show that the matric suction at mid-height of the specimen began to undergo significant changes within the first minute after inundation. The matric suction continued to decrease at a significant rate in the next 6 minutes and approached zero 10 minutes after start of inundation. The matric suction isochrones inferred from the tensiometer readings located at mid-height of the specimen are shown in Fig. 16. It is anticipated that the actual matric suctions at mid-height of the specimen would be a little lower than the tensiometer readings due to the response time of the tensiometer.

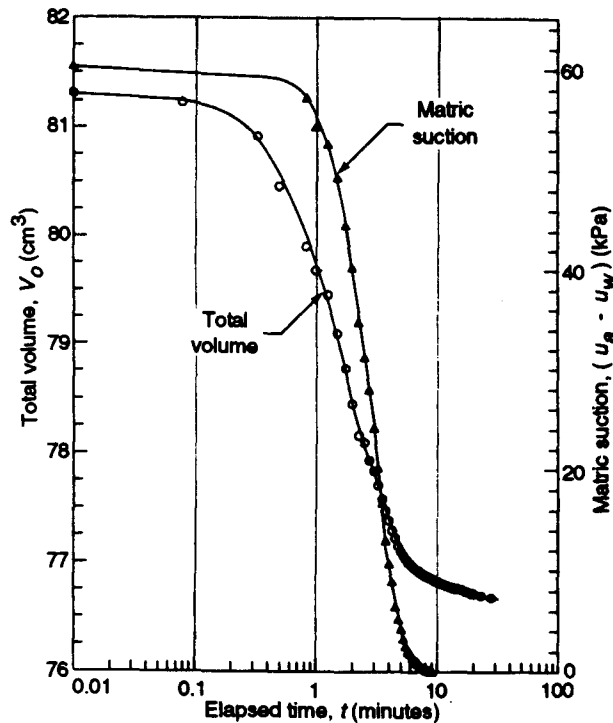


Figure 12. Matric suction and total volume changes with time during inundation in test S1M.

It was observed in Fig. 12 that the total volume of the specimen started to decrease within 6 seconds after inundation. The volume decreased at a slower rate over the next 6 to 7 minutes. The volume then remained almost constant 12 minutes after inundation. The decrease in total volume was observed to have essentially ceased as the matric suction at the center of the specimen approached zero. Since wetting was from both ends of the specimen, the matric suction throughout the entire specimen would have reached a zero value when the matric suction reading at mid-height is zero. This confirms that collapse ceases when the matric suction throughout the specimen reached a zero value. Similar observations were made from the results of tests S2M and S3M. These observations indicate a one-to-one relationship between matric suction changes and total volume changes for the collapsible soils during inundation. The relationship between volume change and the matric suction reading at mid-height of the specimen for tests S1M, S2M and S3M are presented in Fig. 17. The matric suction at mid-height may be used as an *index matric suction* in these cases. The matric suctions are not uniform throughout the specimens. The matric suction has a distribution similar to the isochrones presented in Fig. 16.

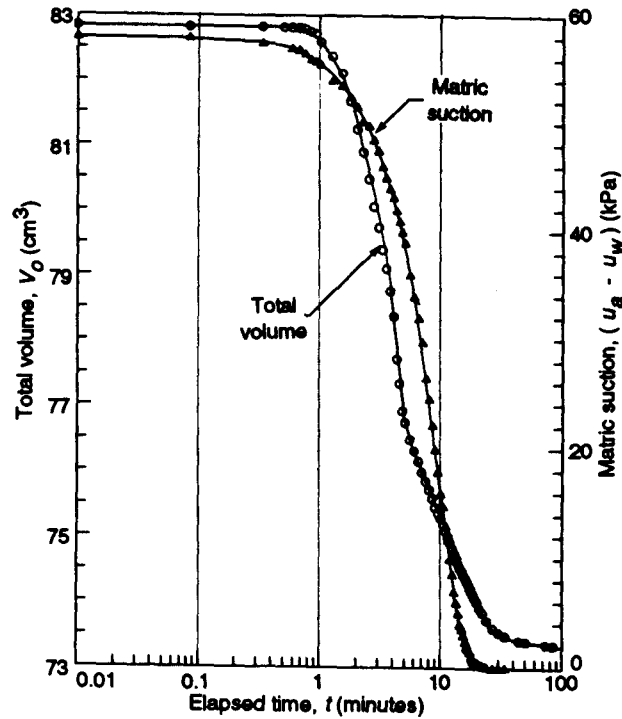


Figure 13. Matric suction and total volume changes with time during inundation in test S2M.

Coefficients of the soil structure volume change with respect to a change in matric suction at mid-height of the specimens can be obtained from Fig. 17. These coefficients are obtained from the slopes of the curves (i.e., the total volume versus matric suction plots) divided by the initial total volume.

Using the endpoint values, (i.e., the total volume change over the total matric suction change) an "overall" coefficient of the soil structure volume change with respect to the change in matric suction could also be computed. The initial matric suction value and the final matric suction value would apply to the total specimen and not just at mid-height of the specimen. The "overall" coefficients of the soil structure volume change for the specimens in tests S1M, S2M and S3M are $9.0\text{E-}04$, $2.0\text{E-}03$ and $2.5\text{E-}03$ $1/\text{kPa}$, respectively.

Test S4M was conducted using a larger specimen in which the changes in matric suction were measured at three different heights. This test was performed to further verify the one-to-one correspondence of the relationship between matric suction changes and the total volume changes during collapse due to wetting. The specimen in

test S4M was allowed access to water from the bottom only. The changes in matric suction with time at the top, middle and bottom of the specimen due to the wetting process, along with the total volume change measurements are shown in Fig. 18. The approximate matric suction isochrones obtained are shown in Fig. 19.

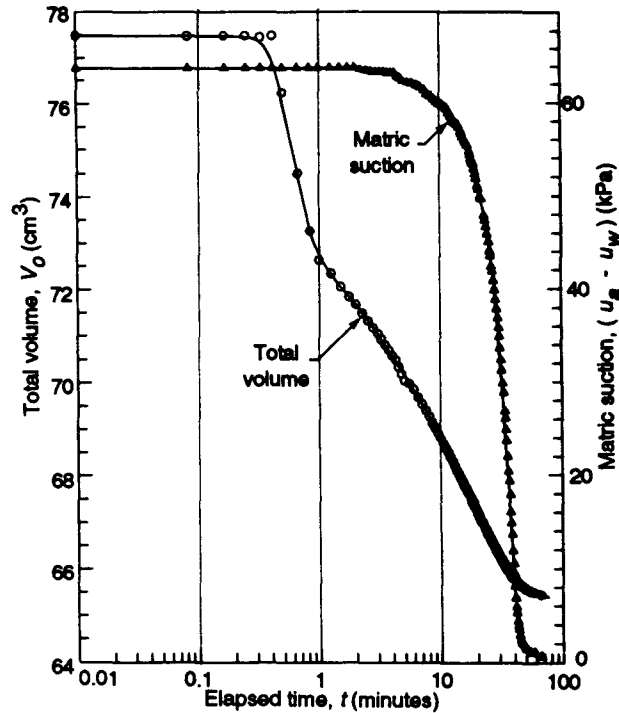


Figure 14. Matric suction and total volume changes with time during inundation in test S3M.

The total volume of the specimen in test S4M remained unchanged during the first 2 minutes after water was allowed through the bottom of the specimen. The total volume decreased significantly between the 2nd and the 60th minute after wetting. The total volume of the specimen decreased at a slow rate from the 60th minute to the 80th minute. No further volume change was observed 80 minutes after the specimen was first allowed access to water.

The volume of the specimen in test S4M began to decrease 2 minutes after water was introduced. The bottom tensiometer readings began to decrease 2.5 minutes after water was introduced. The bottom tensiometer was located at 12.5 mm from the base of the specimen. Thus a decrease in the total volume occurred before a decrease in matric suction was registered by the tensiometer located near the bottom of the specimen. This volume change was due to the collapse of the zone below the bottom tensiometer as a result of a decrease in matric suction from wetting.

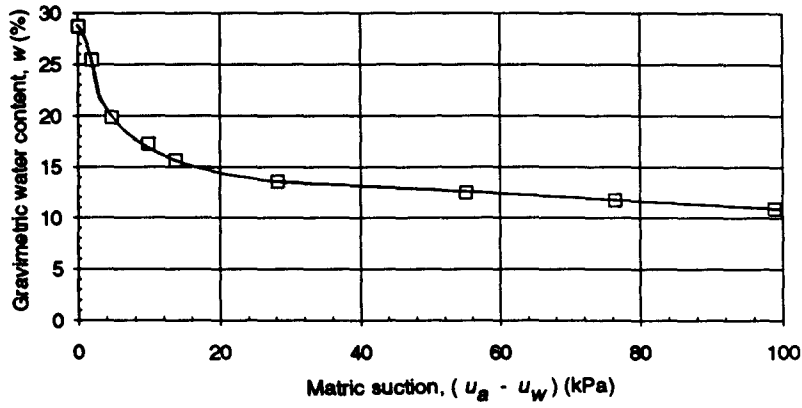


Figure 15. Soil-Water Characteristic Curve for the Indian Head silt

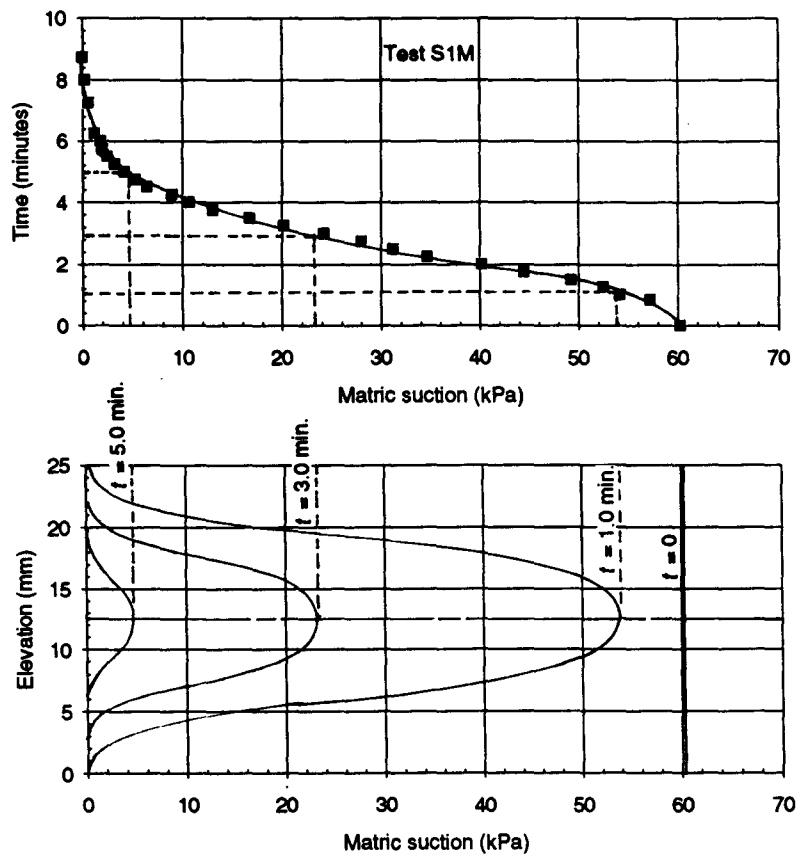


Figure 16. Matric suction isochrones for specimen in test S1M

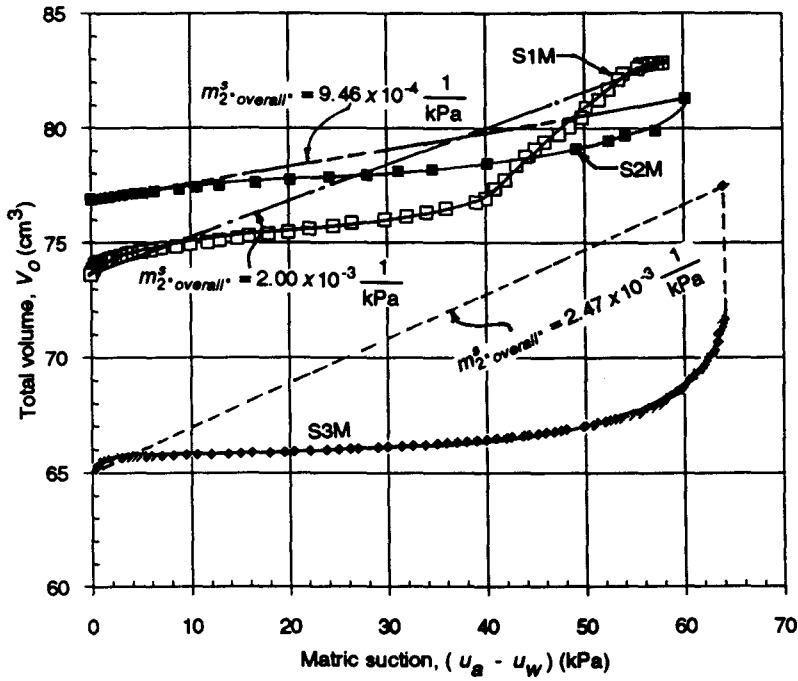


Figure 17. Total volume versus matric suction reading at mid-height of specimen in tests S1M, S2M and S3M.

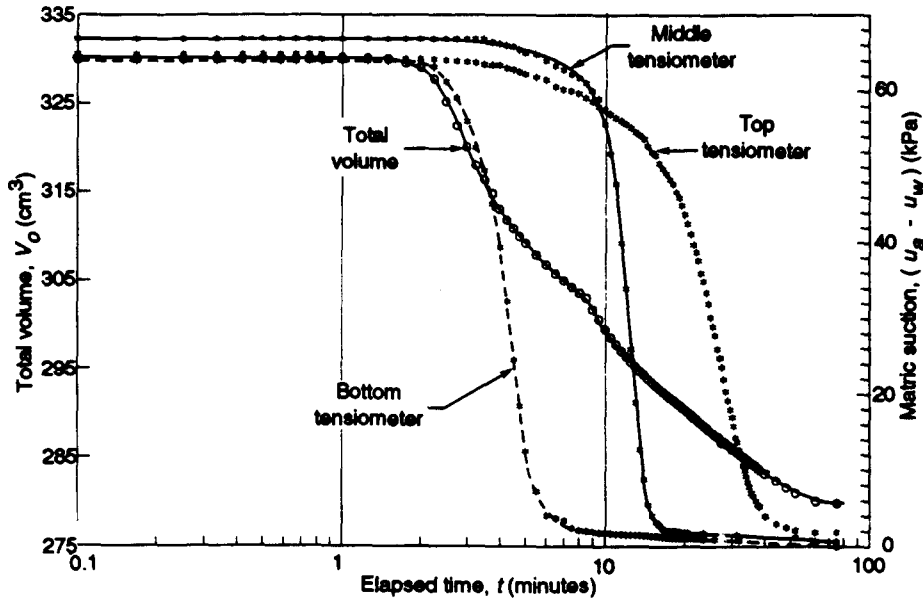


Figure 18. Matric suction and total volume changes versus time during inundation in test S4M.

The initial matric suction of 64 kPa registered by the bottom tensiometer prior to inundation, decreased to zero in about 9.5 minutes after inundation was started. It could be deduced that the collapse of the lower 12.5 mm portion of the specimen was essentially complete in about 9.5 minutes after inundation was started.

The volume of the specimen in test S4M decreased at a continuous rate as the wetting front moved from the bottom to the top of the specimen. The middle tensiometer began to register significant changes in matric suction 5.5 minutes after inundation. The matric suction at the middle tensiometer decreased to zero at a significant rate in the following 12 minutes.

The matric suction at the top tensiometer began a small gradual drop during the first 10 minutes after the specimen was first allowed access to water from the base. This gradual drop in matric suction was due to the accidental application of a small amount of water to the top of the specimen at the beginning of the test. On the whole, the matric suction at the top tensiometer decreases at a much slower rate than the lower two tensiometers. The matric suction at the top tensiometer approached zero about 1 hour after inundation was started. It would appear that gravitational head may have had a significant role in tests S4M.

The matric suction at the top tensiometer approached zero ahead of the time when no further change in total volume was observed. This indicates that the volume changes during the last few minutes were due to the collapse of the region above the top tensiometer as the matric suction in the region above the top tensiometer decreases. The top tensiometer was located 12.5 mm below the top of the specimen.

The experimental results clearly indicate that the total volume of the specimen started to decrease as the matric suction commences to reduce. The volume of the specimen continued to decrease until the matric suction in the entire specimen decreased to zero. This clearly indicates a one-to-one relationship between matric suction and total volume changes during collapse due to inundation.

5. Theoretical Simulations

Theoretical simulations of the matric suction and the total volume changes during collapse were carried out in accordance with the theory presented earlier in the paper. A computer program was written for the water-flow partial differential equation [i.e., Eq. (14)] which was expressed in a finite difference form in Eq. (15).

Relatively steep coefficients of permeability functions would be required in the numerical simulations to produce isochrones similar to those in Figs. 16 and 19. A

steep coefficient of permeability function along with the steep "S" shape form of the Soil-Water Characteristic curve of the soil (Fig. 15) would result in a steep and abrupt function of c_v^w (Fig. 20). Steep abrupt functions of c_v^w would result in difficult instability problems in the numerical solutions. Instead, best-fit solutions to match the experimental results of matric suction and total volume change with time as presented in Figs. 12, 13 and 14 were obtained without a serious attempt to obtain comparable isochrones to those shown in Figs. 16 and 19. The theoretical matric suction isochrones obtained using the best-fit values of c_v^w in the numerical simulations are shown in Fig. 21. The theoretical simulations require the use of a coefficient of consolidation, c_v^w , which varied during inundation. The results of the best simulation obtained for test S1M are compared with the experimental results in Fig. 22. The coefficients of consolidation values used in the simulation of test S1M, as well as the coefficients of consolidation values used in tests S2M and S3M, are shown in Fig. 23.

The varying matric suctions at the bottom, middle and top of the specimen during test S4M, obtained from the theoretical simulations, are compared with the experimental results in Figs. 24, 25 and 26. The coefficient of consolidation was assumed to vary linearly with matric suction, and the values used to obtain the "best-

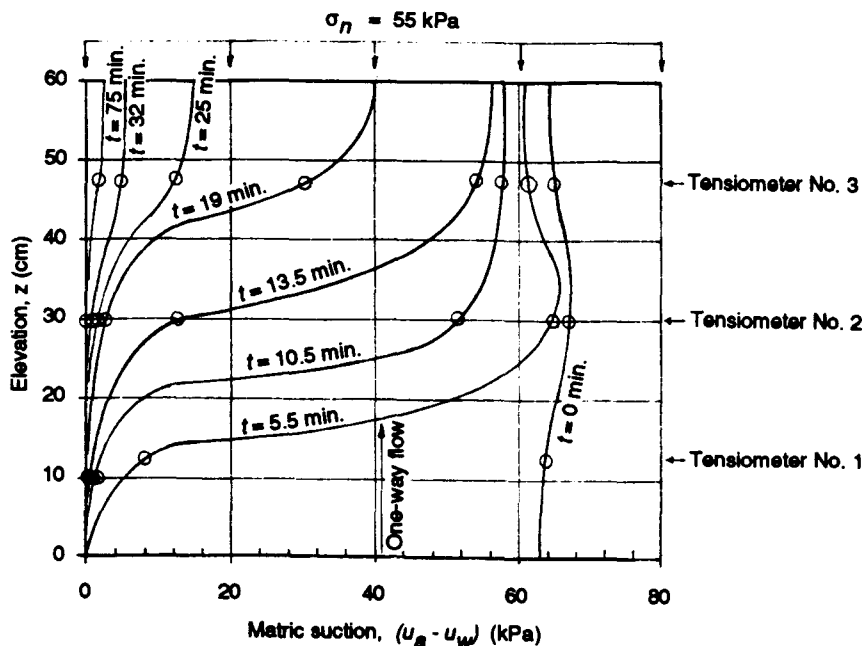


Figure 19. Matric suction isochrones from test S4M.

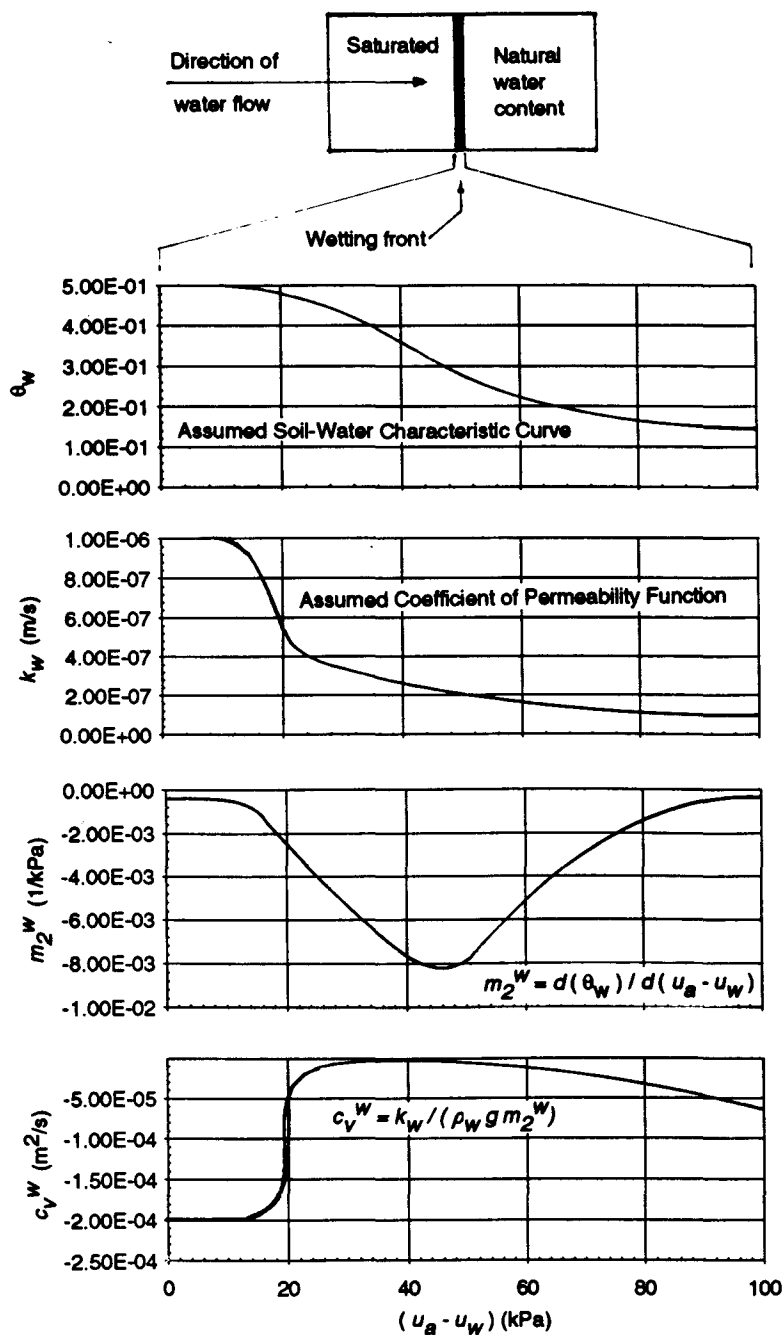


Figure 20. Characteristic functions for m_2^w and c_v^w from assumed functions of θ_w and k_w .

fit" solutions are shown in Fig. 23. Large variations in the coefficient of consolidation and the technique used in programming are the main reasons for numerical instability and scatter in the simulated results shown in Figs. 25 and 26. The use of a steep abrupt consolidation function (Fig. 20) would result in even more difficult problems with numerical instability. The accidental application of a small amount of water to the top of the specimen at the beginning of the test is also partly responsible for the scatter in the simulated results, particularly around the top tensiometer.

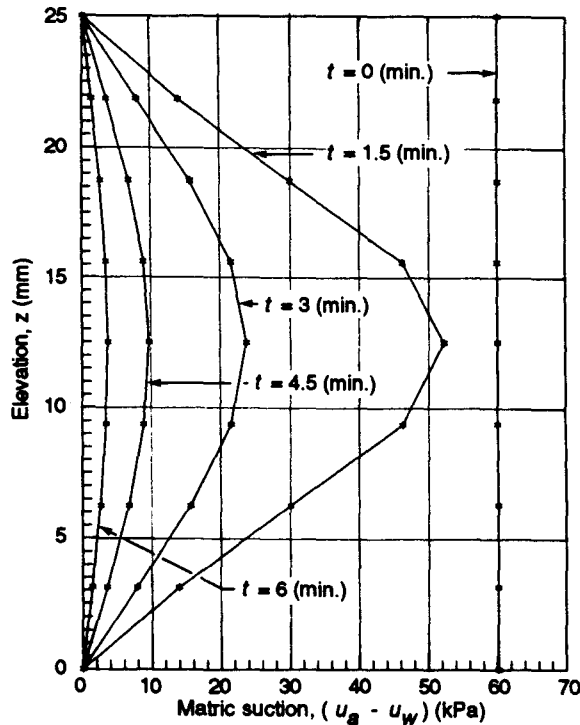


Figure 21. Matric suction isochrones from numerical simulation of test S1M.

Theoretical simulations of the total volume changes were computed using Eq. (2), after the changes in the matric suction of the specimen had been predicted from Eq. (15). Best-fit results of the total volume changes for test S1M were obtained using a constant value of m_2^s throughout the process. A constant value of m_2^s was also used for test S2M. For test S3M, a linearly decreasing m_2^s value was found to better fit the data. The measured total volume changes are compared with the best-fit simulations for test S1M in Fig. 27. The coefficients of volume change used in the theoretical simulations for the total volume changes in tests S1M, S2M and S3M are shown in Fig. 28.

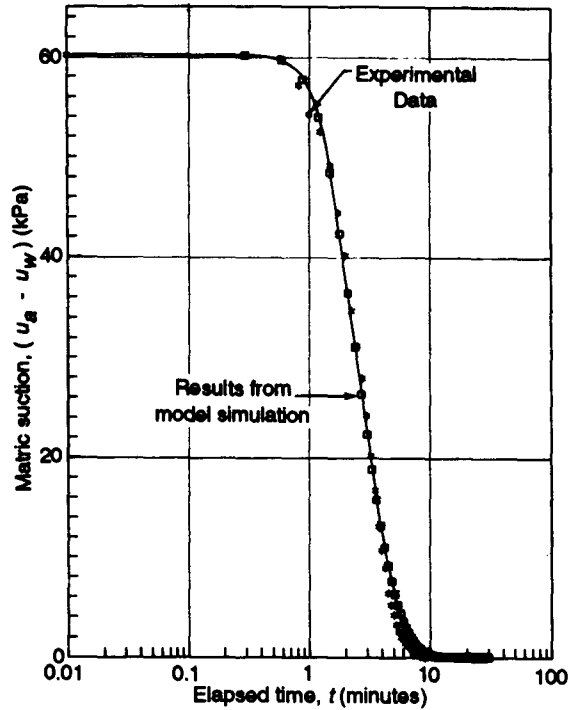


Figure 22. Comparison between the theoretical simulations and experimental results of matric suction changes in test S1M.

For test S4M, the best-fit simulation values were obtained using a linearly decreasing value of m_2^s with respect to matric suction. The comparison between the theoretical simulation and the experimental results from test S4M is shown in Fig. 29. The variation of m_2^s values for the theoretical simulation of test S4M is presented in Fig. 28.

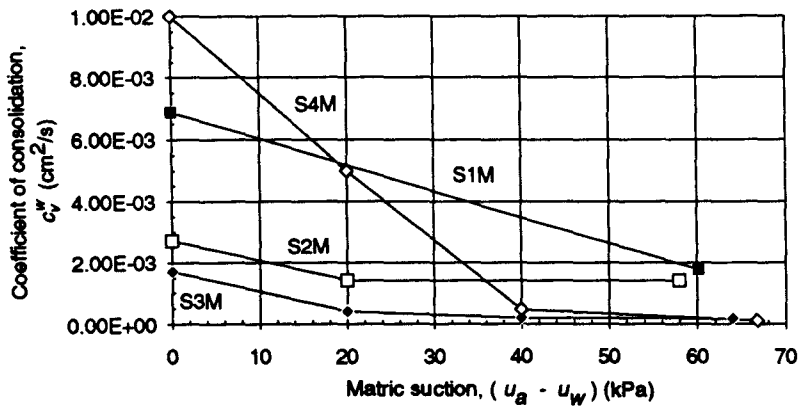


Figure 23. Coefficients of consolidation used in the simulations of tests S1M, S2M, S3M and S4M.

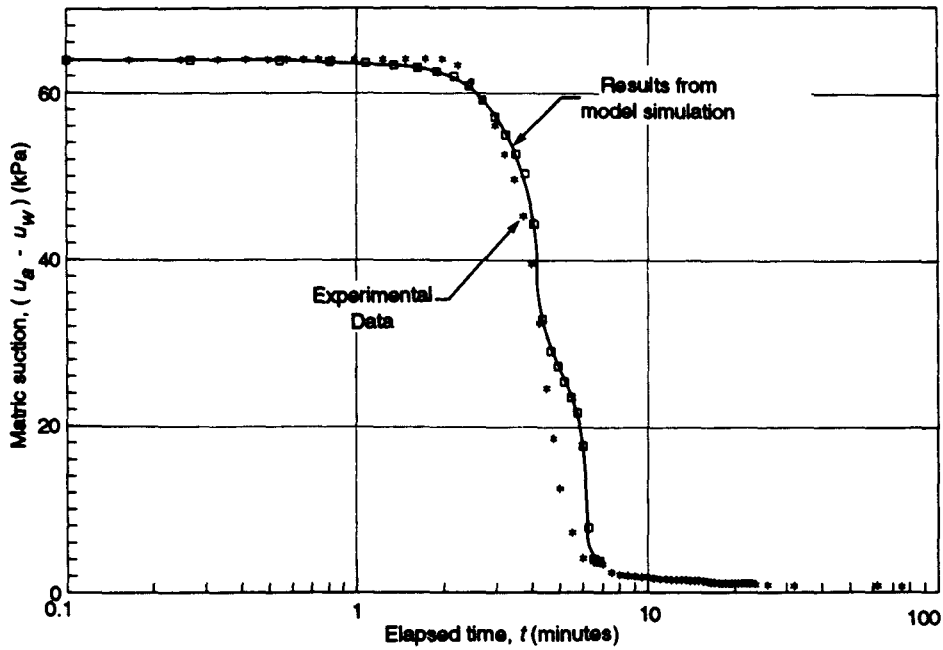


Figure 24. Comparison between the theoretical and experimental results of matric suction changes at the bottom tensiometer location of specimen S4M

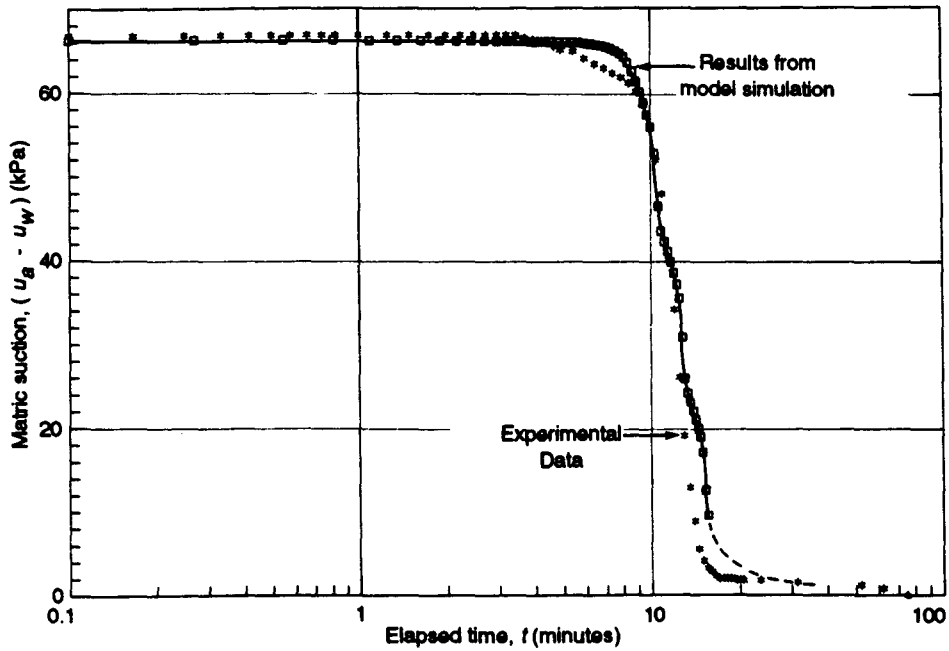


Figure 25. Comparison between the theoretical and experimental results of matric suction changes at the middle tensiometer location of specimen S4M.

The specimens used in tests S1M and S2M had initial dry densities of 1.598 Mg/m^3 and 1.506 Mg/m^3 , respectively. Constant values of m_2^s were obtained from the theoretical simulations for both these specimens. The specimens used in tests S3M and S4M had initial dry densities of 1.406 Mg/m^3 and 1.394 Mg/m^3 , respectively. Linearly decreasing values of m_2^s were obtained from the theoretical simulations for both these specimens in test S3M and S4M.

It appears that constant m_2^s values could be used in the simulations for higher density specimens (i.e., specimens having a dry density equal to or higher than 1.5 Mg/m^3). For the specimens with lower dry densities, linearly decreasing m_2^s values with respect to matric suction appear to better fit the theoretical simulations.

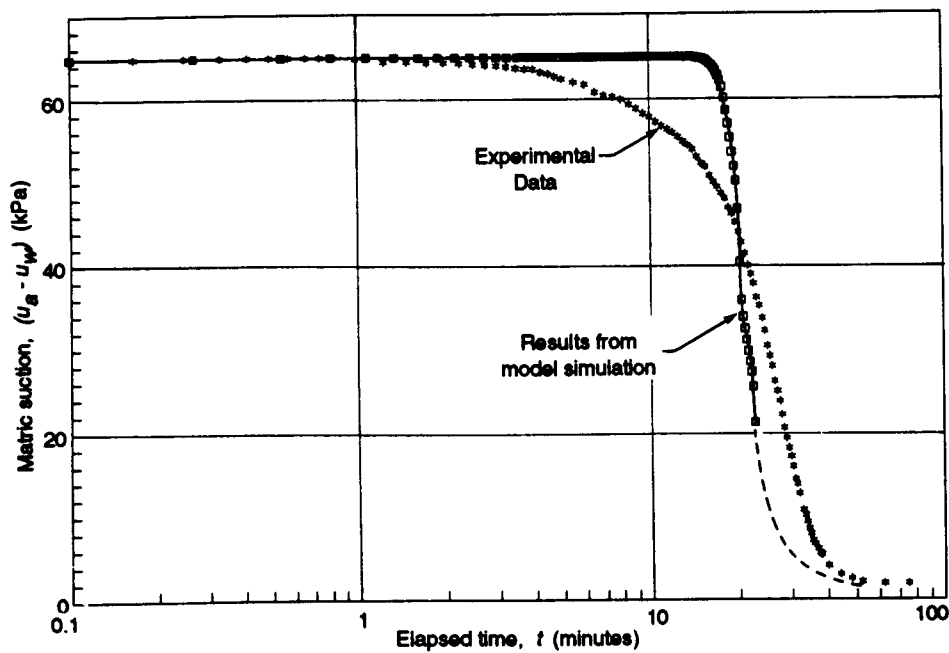


Figure 26. Comparison between the theoretical and experimental results of matric suction changes at the top tensiometer location of specimen in test S4M.

Since collapse is confined within the wetted zone and since the wetting of the soil is progressive due to the advancement of the wetting front, collapse is, therefore, occurring in each instance of time in newly wetted material. Thus a constant value of m_2^s would appear reasonable. That is, material which has already collapsed will not

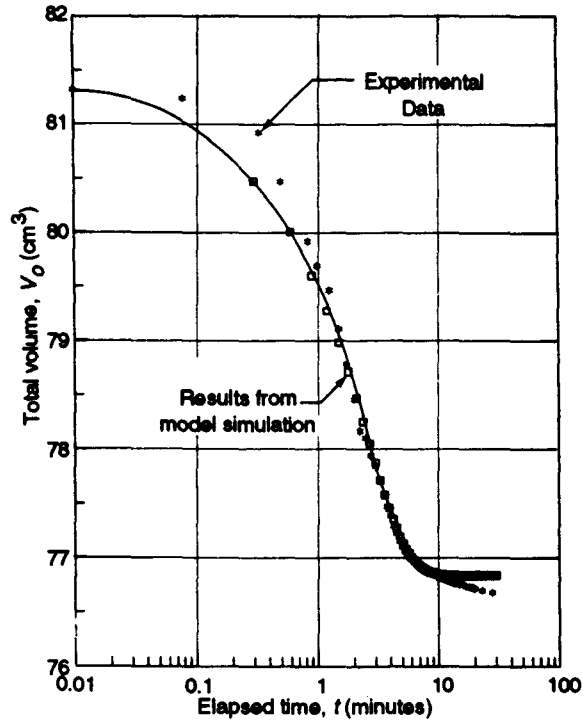


Figure 27. Comparison between the theoretical and experimental results of total volume changes in test S1M.

undergo further collapse as the wetting front advances. In the lower density specimens, however, the collapse of the initially wetted zone may have a significant impact on the soil ahead of the wetting zone due to the greater collapsibility and the looseness of the structure of the soil. Thus, resulting in a linearly decreasing m_2^s in the lower density specimens as matric suction decreases.

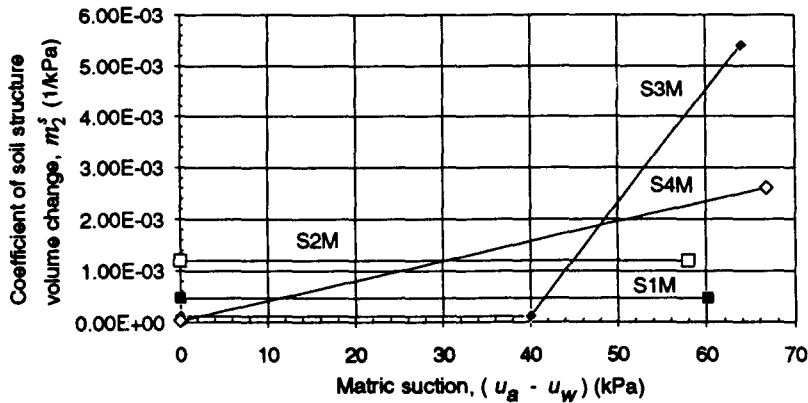


Figure 28. Coefficients of structure volume change used in the numerical simulations.

The plots of total volume versus matric suction at mid-height of specimen presented in Fig. 17 for specimens in tests S1M, S2M, and S3M, respectively, also show that the change in total volume with a decrease in matric suction at mid-height is increasingly more nonlinear as the dry densities of the specimens decrease. The specimen in test S1M shows approximately two linear stages of change in total volume as the matric suction at mid-height decreases. The total volume change from a matric suction value of 60 kPa to 40 kPa is more rapid than the total volume change from a matric suction value of 40 kPa to 0 kPa. The specimen in test S2M shows a gradual and approximately linear change in total volume as the matric suction at mid-height decreases. The lower density specimen in test S3M show a sharp drop in total volume when the specimen first experienced wetting. The specimen continue to show rapid but decreasing smaller changes in total volume down to a matric suction of about 50 - 55 kPa. Below 50 kPa, the specimen continues to show an additional small total volume change as the matric suction at mid-height continues to decrease to zero.

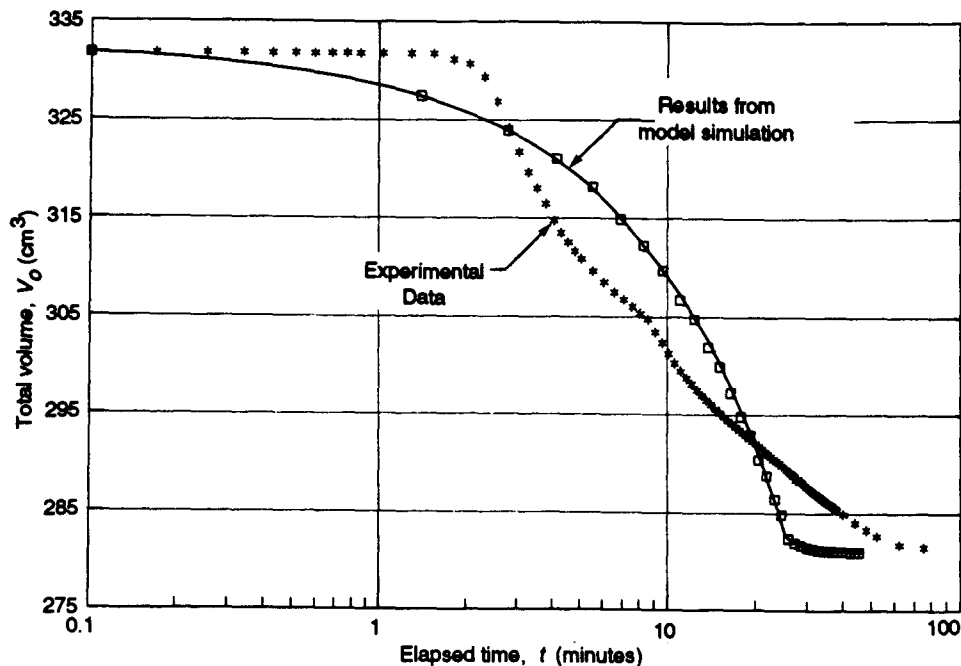


Figure 29. Comparison between the theoretical and experimental results of total volume changes at the top tensiometer location of specimen in test S4M.

6. Conclusions

The collapse of an uncemented, dry collapsible soil is due to the loss in the normal stress between soil particles leading to shear failure as a result of a reduction of matric suction from wetting. Laboratory test results show that there is a one-to-one correspondence between volume change due to collapse and the reduction in matric suction from wetting.

Soil mechanics principles developed for unsaturated soils can be used to describe the collapse behavior of an uncemented, dry collapsible soil. Flow and volume change formulations derived in terms of the two stress state variables (i.e., $(\sigma_y - u_a)$ and $(u_a - u_w)$) appear to describe adequately the collapse mechanism. Numerical modeling using the formulations derived from soil mechanics principles developed for unsaturated soils fitted the experimental results well.

Experimental results confirm that the collapse of an uncemented, dry collapsible soil is a transient process. There exists a matric suction change with time relationship due to the process of wetting. There exists a matric suction and total volume change relationship during the collapse process.

7. Acknowledgments

The authors wish to acknowledge the contributions of Mr. Rambabu Tadepalli. The experimental work on which this paper was based were conducted by Mr. Tadepalli as part of the requirements for a M.Sc. thesis at the University of Saskatchewan, Saskatoon, Saskatchewan, Canada.

7. References

1. Bear, J. (1972) *Dynamics of Fluids in Porous Media*, American Elsevier Publishing Company, Inc. New York.
2. Fredlund, D.G., and Rahardjo, R. (1993) *Soil Mechanics for Unsaturated Soils*, John Wiley & Sons, Inc., New York.
3. Fredlund, D.G., and Morgenstern, N.R. (1977) Stress state variables for unsaturated soils, *ASCE J. Geotech. Eng. Div. GT5* **103**, pp. 447-466.
4. Rubin, J. (1966) Numerical analysis of ponded rainfall infiltration, *I.A.S.H. Symp. Water in Unsaturated Zone*, Wageningen, The Netherlands, pp. 440-451.
5. Tadepalli, R. (1990) *The Study of Collapse Behavior of Soils during Inundation*, M.Sc. thesis, University of Saskatchewan, Saskatoon, Saskatchewan, Canada, 276 pp.
6. Tadepalli, R., and Fredlund, D.G. (1991) The Collapse Behavior of a Compacted Soil During Inundation, *Canadian Geotechnical Journal*, **28**, pp. 477-488.

7. Tadepalli, R., Fredlund, D.G., and Rahardjo, H. (1992) Soil Collapse and Matric Suction Change, *Proceedings of the 7th International Conference on Expansive Soils (Dallas, Texas), August 3-5, 1*, pp. 286-291.
8. Tadepalli, R., Rahardjo, H., and Fredlund, D.G. (1992) Measurements of Matric Suction and Volume Changes During Inundation of Collapsible Soils, *Geotechnical Testing Journal, ASTM, GTJODJ*, **15**, No.2, pp. 115-122.